HHS Public Access

Author manuscript

J Neurosci Res. Author manuscript; available in PMC 2020 July 01.

Published in final edited form as:

J Neurosci Res. 2020 January ; 98(1): 168–178. doi:10.1002/jnr.24478.

Annexin A1 Attenuates Neuroinflammation through FPR2/p38/COX-2 Pathway after Intracerebral Hemorrhage in Male Mice

Yan Ding[1], **Jerry Flores**[1], **Damon Klebe**[1], **Peng Li**[1], **Devin W. McBride**[2], **Jiping Tang**[1], **John H. Zhang**[1,3]

[1]Department of Basic Sciences, School of Medicine, Loma Linda University, Loma Linda, CA, 92350

[2]The Vivian L. Smith Department of Neurosurgery, McGovern Medical School, University of Texas Health Science Center at Houston, Houston, TX 77030

[3]Departs of Anesthesiology, Neurology and Neurosurgery, Loma Linda University, Loma Linda, CA 92350

Abstract

Spontaneous intracerebral hemorrhage (ICH) is the deadliest stroke subtype and neuroinflammation is a critical component of the pathogenesis following ICH. Annexin A1-FPR2 signaling has been shown to play a protective role in animal stroke models. This study aimed to assess whether Annexin A1 attenuated neuroinflammation and brain edema after ICH and investigate the underlying mechanisms. Male CD-1 mice were subjected to collagenase-induced ICH. Annexin A1 was administered at 0.5 hour after ICH. Brain water content measurement, short-term and long-term neurobehavioral tests, Western blot and immnunofluorescence were performed. Results showed that Annexin A1 effectively attenuated brain edema, improved short-term neurological function and ameliorated microglia activation after ICH. Annexin A1 also improved memory function at 28 days after ICH. However, these beneficial effects were abolished with the administration of FPR2 antagonist Boc-2. Furthermore, AnxA1/FPR2 signaling may confer protective effects via inhibiting p38-associated inflammatory cascade. Our study demonstrated that Annexin A1/FPR2/p38 signaling pathway played an important role in attenuating neuroinflammation after ICH and that Annexin A1 could be a potential therapeutic strategy for ICH patients.

Graphical Abstract

Corresponding Author: John H. Zhang, Risley Hall Rm 219, 11041 Campus St, Loma Linda, CA 92350, Tel: 909-558-4723, Fax: 909-558-0119, johnzhang3910@yahoo.com.

Author Contributions

All authors had full access to all the data in the study and take responsibility for the integrity of the data and the accuracy of the data analysis. Study concept and design: Y.D. and J.F. Acquisition of data: Y.D., J.F., D.K., P.L. Analysis and interpretation of data: Y.D., J.F., D.K., J.T., and J.H.Z. Drafting of the manuscript: Y.D., and J.F. Statistical analysis: D.W.M., Y.D. and D.K. Manuscript revision: Y.D., D.W.M. and J.F. Obtained funding: J.T. and J.H.Z. Study supervision: J.H.Z.

Conflicts of Interest Statement

None

Data Accessibility

All authors have full access to all the data in the study and take responsibility for the integrity of the data and the accuracy of the data analysis. Original data or protocols will be available from the corresponding author upon reasonable request.

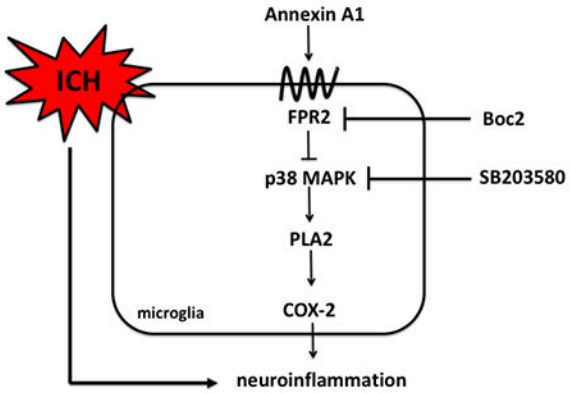

Keywords

Annexin A1; intracerebral hemorrhage; neuroinflammation; p38 MAPK

Introduction

Spontaneous intracerebral hemorrhage (ICH) is the deadliest and least treatable stroke subtype, affecting approximately 80,000 individuals in the United States (Go et al., 2014). The extravasated blood products trigger a series of life threatening events, leading to formation of brain edema, brain swelling, and possibly death (Dang et al., 2017; Jiang et al., 2017; Strbian et al., 2008). However, no therapies have proven effective in improving the acute and chronic outcomes following ICH. Mounting evidence has shown that inflammation, which begins immediately after the formation of hematoma, is one of the crucial contributors of ICH-induced secondary brain injury. Activated microglia and infiltrating leukocytes have been implicated as essential factors of the neuroinflammatory response promoting disease progression(Aronowski et al., 2011). Thus, an anti-inflammatory medication is expected to reduce brain edema and microglial activation, thereby optimizing recovery following ICH.

N-formyl peptide receptors (FPR) belong to a family of G-protein-coupled receptors that are expressed on microglia in the central nervous system(Cui et al., 2002). Stimulation of the n-formyl peptide receptor 2 (FPR2) by Annexin A1 (AnxA1) attenuates inflammation and immune cell activation in preclinical models of inflammatory disease (Bena et al., 2012; Gavins, 2010; Gavins & Hickey, 2012; Gavins, Hughes, et al., 2012; McArthur et al., 2010). A previous study demonstrated that AnxA1-FPR2 signaling decreased leukocyte adhesion to cerebral endothelial cells, reduced proinflammatory cytokine levels as well as infarction volumes in a rodent model of focal brain ischemia(Gavins et al., 2007).

Another human microarray study showed that among all the anti-inflammatory factors, Annexin A1 gene is the most significantly induced in the perihematomal tissues from ICH patients, indicating an endogenous protective mechanism(Carmichael et al., 2008). Thus, to investigating the protective mechanisms underlying FPR2 stimulation may uncover novel therapeutic modalities for ICH.

Previous research from our laboratory has shown that p38 MAPK is activated in response to ICH and that p38-induced stimulation of PLA_2/COX-2 may be involved in the injury progression following ICH (Ma et al., 2011). Specifically, upstream inflammatory stimuli activates PLA_2 and consequently increases the production of arachidonic acid, which is converted by cyclooxygenase-2 (COX-2) to pro-inflammatory prostaglandins(Degousee et al., 2001). However, the upstream regulator of p38 MAPK is largely unknown. In this study, we aimed to investigate whether p38 MAPK was a potential target of AnxA1/FPR2 signaling pathway.

Thus, we hypothesized that Annexin A1 attenuated neuroinflammation and brain edema following ICH and that this protective effect was mediated by FPR2/p38 MAPK/COX-2 pathway.

Methods

Animals and surgical procedures

All animal procedures for this study were approved by the Animal Care and Use Committee at Loma Linda University and complied with the US National Research Council's Guide for the Care and Use of Laboratory Animals, the US Public Health Service's Policy on Humane Care and Use of Laboratory Animals, and the Guide for the Care and Use of Laboratory Animals. Animal use and procedures were reported according to ARRIVE guidelines. Animal use and animal numbers of each experiment were outlined in Supplemental Table 1. Eight-week-old male CD1 mice (weight 35-40g; Charles River, Wilmington, MA) were housed at room temperature of 25°C with a 12-hour light cycle/12-hour dark cycle. Animal surgeries were performed between 8am and 12pm. Animals had access to food and water *ad libitum*.

We chose to focus on the male gender in this study since several clinical studies have indicated that male sex could be one of the risk factors for spontaneous ICH(Marini et al., 2017; Roquer et al., 2016). In addition, estrogen has been shown to be protective in stroke(Faber et al., 2017; Lee et al., 2018; Nakamura et al., 2005). Naïve female mice at this age might not represent a large clinical population.

For collagenase ICH induction, mice were intraperitoneally injected with ketamine (100 mg/kg) and xylazine (10 mg/kg) (2:1 v/v,) and positioned prone in a stereotactic head frame (Kopf Instruments, Tujunga, CA, USA). A cranial burr hole(1mm) was made close to the right coronal suture, 2.2 mm lateral to the midline and 0.2 mm posterior to Bregma. To perform the ICH model, a 27-gauge syringe (Hamilton Company, Reno, NV) with bacterial collagenase (VII-S, Sigma-Aldrich, St Louis, MO) was inserted stereotactically into the right basal ganglia coordinates and lowered 3.5 mm ventrally through the burr hole. The syringe was then connected onto a micro-perfusion pump (Harvard Apparatus, Holliston, MA). Bacterial collagenase (0.075 U dissolved in 0.5μL of PBS) was infused into the brain over 2 minutes at a rate of 0.25 mL/min with a microinfusion pump. Sham operated mice were subjected to needle insertion only. After completed injection, the needle was left in place for an additional 5 min to prevent backflow.

Intracerebroventricular (i.c.v) drug administration was performed as in our previous study(Chen et al., 2018). Briefly, the 26-gauge needle of a 10μl Hamilton syringe was inserted into the left lateral ventricle (the contralateral side of hemorrhage) through a cranial burr hole at the coordinates relative to Bregma: 0.3mm posterior; 1.0 lateral; and 2.3mm deep. Then drugs were infused by a microinfusion pump at a rate of 0.667μl/min over a period of 3 minutes. The needle was left for an additional 5 minutes after the infusion and then removed over a three-minute period. The burr hole was sealed with bone wax.

After completing ICH surgeries or i.c.v. injections, buprenorphine in 0.5 ml of normal saline was given to each mouse by subcutaneous injection before surgical recovery to avoid post-surgical dehydration and pain. Animals were placed on a heated blanket and observed closely for recovery. We then closely monitored the body weight and feeding behavior of the experimental animals. Mice were monitored closely every 20 minutes during the first 2 hours and then once daily till sacrifice.

Animals were excluded when 1) the Garcia Score of ICH animals was the same as Sham animals; 2) hematoma was not observed when we sacrificed the animals, as shown in Supplemental Table 1.

Experimental Protocols

Experiment 1.—Temporal expression profile of Annexin A1 after ICH. 30 mice were randomly divided into six groups: Sham (n=6), 12 hours after ICH (n=6), 24 hours after ICH (n=6), 72 hours after ICH (n=6) and 7 days after ICH (n=6). Western blot analysis was used to detect their expression in the ipsilateral/right hemisphere of each group.

Experiment 2.—Modified Garcia tests and brain edema measurement. Experimental groups were Sham (n=6), ICH+Vehicle (n=6), ICH+AnxA1 (0.1 μg/animal, n=6) and ICH +AnxA1 (0.5μg/animal, n=6) for the 24-hour time point. Garcia tests were performed and the same animals were used for brain water content measurement. The more optimal dose (0.5μg/animal) was chosen for the 72-hour time point. Experimental groups include Sham (n=6), ICH+Vehicle (n=6), ICH+AnxA1 (0.5μg/animal, n=6) for 72-hour time point. Garcia tests were performed and the same animals were used for brain water content measurement.

Experiment 3.—Microglial activation. Experimental groups were Naïve (n=6), Sham (n=6), ICH+Vehicle (n=6) and ICH+AnxA1 (n=6). Animals were sacrificed at 24 hours after ICH for immunofluorescence.

Experiment 4.—Long-term memory function assessment. Experimental groups were Sham (n=10), ICH+Vehicle (n=10) and ICH+AnxA1 (n=10). Water maze test was performed between Day 25 and Day 28 after ICH.

Experiment 5.—Mechanistic study of Annexin A1 signaling. Experimental groups were Sham (n=6), ICH+Vehicle (n=6), ICH+AnxA1 (n=6), ICH+AnxA1+Boc2 (n=6) and ICH +Boc2+SB203580 (n=6). Samples were collected 24 hours after ICH for Western blot analysis.

Drug Administration

Recombinant human Annexin A1 protein (AnxA1, R&D Systems) and the FPR2 antagonist N-t-butyloxycarbonyl-Phe-DLeu-Phe-DLeu-Phe (Boc2; MP Biomedicals), and SB203580 (an inhibitor of p38 MAPK, Santa Cruz Biotechnology) were dissolved in 2μl sterile PBS. AnxA1 was administered i.c.v. at 0.5 hour after ICH induction. Boc2 (0.8μg/mouse) and SB203580(0.4μg/mouse) was given 1 hour before ICH induction via intracerebroventricular injection. Vehicle animals received the same volume of PBS injection. All drugs were administered to the contralateral side of hemorrhage to avoid interaction with collagenase.

Behavioral Assessment

Garcia tests—The sensorimotor Garcia tests were conducted in a blinded fashion to assess neurological outcomes in mice at 24 and 72 h after surgery (J. H. Garcia et al., 1995). The Garcia Test has been modified and consisted of 7 individual tests, namely spontaneous activity, axial sensation, vibrissae proprioception, limb symmetry, lateral turning, forelimb outstretching, and climbing. A score of 0 (worst performance) to 3 (best performance) was given for each sub-test and a total Garcia score was calculated as the sum of all sub-tests (maximum score of 21).

Morris water maze—Spatial learning ability was evaluated by Morris water maze between Day 25 and Day 28 after ICH as previously described (Chen et al., 2018). Mice were released in a metal pool (110 cm diameter) filled with water and were allowed to swim to find a submerged platform (11 cm diameter). The location of platform and starting direction were designed according to a previous publication (Bromley-Brits et al., 2011). One day before Block 1, the cued water maze test was performed which assessed any sensorimotor and/or motivational deficits that could potentially affect the performance during the spatial water maze test. In the cued test, the animal was allowed to swim and find the platform, which was made visible 5mm above the surface of water. If the animal could not find the platform by the end of each trial, they were guided to the platform and stayed on the platform for 5 seconds. The location of the platform was changed in each trial. Next, the spatial water maze test was performed over 4 days to test for spatial learning and memory. In the spatial test, the animal swam to find the platform, which will be submerged one centimeter below the surface of the water. The location of the platform was kept in the same place throughout the four blocks. At the end of Block 4, the platform was removed. Probe Trial was performed to record the percentage of the time (60 seconds in total for each animal) spent in the target quadrant in which the platform used to be. Block 4 and Probe trial were conducted on the same day, with a five-hour period in between. An overhead camera with a computerized tracking system (Noldus Ethovision; Noldus, Tacoma, WA) will record the swim path and measure the swim distance, swim speed and time spent in probe quadrant.

Measurement of brain water content

Brain water content (edema) was evaluated via the wet-weight/ dry-weight method, as previously described (Chen et al., 2018). Briefly, animals were sacrificed at 24 or 72 h after ICH, brains were immediately removed and divided into 4mm-thick sections. Each brain sections were further divided into ipsilateral cortex (Ipsi-CX) and basal ganglia (Ipsi-BG)

and contralateral cortex (Cont-CX) and basal ganglia (Cont-BS). The tissue was then dried at 100°C for 24 hours to determine the dry weight (DW). All samples were weighed on an analytical microbalance (APX-60, Denver Instrument, Bohemia, NY). Brain water content was calculated as (wet weight–dry weight)/wet weight×100%.

Western Blotting

Western Blotting was performed as described previously (Chen et al., 2018; Ma et al., 2011). Mice were sacrificed at 24h after ICH. Right brain hemispheres were collected and stored at −80°C immediately until analysis. Protein lysates were obtained by gently homogenizing tissues in RIPA lysis buffer (Santa Cruz Biotechnology), followed by centrifugation at 14,000 g at 4°C for 30 minutes. Equal amounts of protein (30μg) were loaded on an SDS-PAGE gel. After being electrophoresed and transferred to a nitrocellulose membrane, the membrane was blocked in milk and incubated overnight at 4°C with the primary antibodies. The primary antibodies were rabbit polycolonal anti-AnxA1 (ThermoFisher Scientific), rabbit phosphorylated p38 (p-p38, Cell Signaling Technology), rabbit anti-p38 MAPK (Cell Signaling Technology), rabbit polyclonal anti-tumor necrosis factor-α (TNF-α, Abeam) and rabbit monoclonal anti-interleukin-1β (IL-1β, Cell Signaling Technology), rabbit polyclonal anti-cytosolic phospholipase A2 (cPLA2, Abeam) and rabbit polyclonal anti-cyclooxygenase 2 (COX-2, Abeam). Specific antibody information was listed in Table 1. Nitrocellulose membranes were incubated with appropriate secondary antibodies (Santa Cruz Biotechnology) for 1 hour at room temperature. Immunoblots were then probed with an ECL Plus chemiluminescence reagent kit (Amersham Biosciences, Arlington Heights, IL, USA) and visualized with the imaging system (Bio-Rad, Versa Doc, model 4000). The data were analyzed by the software Image J (NIH). In addition, specificity of the antibodies was tested using whole gels and membranes. The whole gel images were exposed and demonstrated in Supplemental Figure 1.

Immunofluorescence

At 24 hours after ICH, mice were perfused under deep anesthesia with cold PBS (pH 7.4), followed by infusion of 4% formalin. The brains were then removed and fixed in formalin at 4°C overnight and then were dehydrated with 30% sucrose in PBS (pH7.4) until they sank to the bottom. The frozen coronal slices (10mm thick) were then sectioned with cryostat (CM3050S; Leica Microsystems, Bannockburn, IL, USA). Immunohistochemistry was performed as previously described(Chen et al., 2018). Briefly, samples were permeabilized with 0.3% Triton-X-100, blocked with 5% donkey serum and incubated overnight at 4°C with primary antibody anti-Iba-1 (1:100, Abeam). Sections were then incubated with secondary antibody for two hours at room temperature and visualized with a fluorescence microscope (Leica Microsystems, Germany). We chose three regions of interest (ROIs) in the perihematoma area on each section, as illustrated in Figure 3. Six sections were imaged to represent each animal and each experimental group had six animals. Values obtained from one animal were averaged to represent each animal and values obtained from six different animals were average to represent each experimental group. Quantitative analysis was conducted using ImageJ (NIH) by an investigator who was blinded to the experimental groups.

Statistical Analysis

Animals were numbered and randomized into different experimental groups using Excel. Samples size of each experiment was determined according to previous research. All the experimental groups were blinded to the scientists performing behavioral tests. Non-parametric behavioral data were statistically analyzed using Kruskal–Wallis test, followed by Dunn's test. Parametric data were first tested for normal distribution. Multiple comparisons of parametric data were statistically analyzed with one-way AVONA followed by Tukey's test. Latency of Morris water maze data were analyzed with two-way ANOVA followed by Tukey's test. Data were expressed as mean ± SD. P value of < 0.05 was considered statistically significant. All statistical analyses were performed using the software Graphpad Prism6.

Results

Endogenous Annexin A1 level peaked at 24 hours after ICH

Western blot was performed to determine the expression profile of AnxA1 at 12, 24, 72 hours and 7 days after ICH. Endogenous AnxA1 level reached the peak level at 24 hours ($F(4,25)=60.66$, total n=30; $p<0.0001$) and still remained higher than Sham at 72 hours. At 7 days after ICH, AnxA1 expression returned to the baseline (Figure 1).

Annexin A1 improved neurological function and attenuated brain edema at 24 hours and 72 hours after ICH

Two doses of AnxA1 (0.1 μg/mouse and 0.5μg/mouse) were administered i.c.v. at 0.5 hour after ICH. To evaluate the behavioral deficits after ICH, the Garcia test was conducted at 24 hours post-ictus. Vehicle-treated mice demonstrated significant neurological deficits compared with sham mice (total n=24; p=0.0002). Treatment with lower dose of AnxA1 (0.1 μg/mouse) did not improve the neurological outcomes compared with vehicle-treated animals. However, treatment with high-dose AnxA1 (0.5μg/mouse) significantly improved neurobehavioral function as shown in the Garcia score at 24 hours (Figures 2A). Thus, we chose the higher dose for the 72-hour assessment. This treatment regimen of AnxA1 significantly improved the neurological outcomes compared to the vehicle group at 72 hours in modified Garcia tests (total n=18; $p<0.0001$, Figure 2B). Brain edema was measured as brain water content. At both 24 hours and 72 hours after ICH, higher dose of AnxA1 significantly ameliorated brain edema in the ipsilateral basal ganglia part ($F(3,20)=21.85$, n=24, $p<0.0001$ at 24 hours; $F(2, 15)=9.671$, n=18, p=0.002 at 72 hours). Lower dose of AnxA1 did not significantly reduce the brain water content compared to the vehicle group. Other parts of the brain had comparable water content among all the experimental groups (Figure 2C and 2D). Thus, we chose the higher dose of AnxA1 (0.5μg/mouse) for the following studies.

In addition, to test whether saline injections alone would cause any effects, we injected the same volume of saline to sham-operated animals and measured the Garcia score and brain water content at 24 hours after the sham operation. Results showed that saline injections alone did not alter neurobehavioral score or brain edema (Supplemental Figure 2). Thus, we

presume that saline injections would not induce neuroinflammation or impinge on AnxA1-FPR2 signaling.

Annexin A1 attenuated microglial activation at 24 hours after ICH

Microglia morphology was assessed using immunofluorescence staining of microglia marker Iba-1 in the perihemotoma areas of the brain. At 24 hours after ICH, microglia were activated as demonstrated by more Iba-1 positive cells, bigger soma size, increased Iba-1 fluorescence intensity and shorter process length than sham animals. AnxA1 treatment effectively reduced the Iba-1 positive cells and the soma size of microglia compared to vehicle-treated animals ($F(3, 20)=99.37$, total n=24, $p<0.0001$ in Iba-1 positive cell numbers; $F(3, 20)= 191.2$, total n=24, $p<0.0001$ in soma size; $F(3, 20)= 110.5$, $p<0.0001$ in Iba-1 intensity; $F(3, 20)=64.21$, total n=24, $p<0.0001$ in total process length per cell). Nevertheless, Iba-1 might not be a sufficient marker to distinguish microglia and macrophages. We also included naïve animals in this experiment to assess whether the surgery itself elicited microglial activation or macrophage infiltration. Our data showed that there were no significant differences between naïve and sham-operated animals, suggesting that the sham surgery alone did not induce microglia activation or macrophage infiltration (Figure 3).

Annexin A1 improved spatial learning function at 4 weeks after ICH

To assess whether ICH also led to cognitive impairment in the long term, Morris water maze was conducted to test the animals' spatial learning ability. Each block was performed on a different day over a course of four days. Escape latency was comparable among all the experimental groups in the first two blocks. In Block 3 and Block 4, vehicle animals took significantly longer time to find the platform than sham animals, indicating impaired memory function (interaction $F(6,108)=3.084$, total n=30, $p=0.008$; different time blocks $F(3,108)=120.2$, total n=30, $p<0.0001$; different treatments $F(2, 108)=14.86$, total n=30, $p<0.0001$). AnxA1-treated group demonstrated significantly shorter escape latency in Block 3 and Block 4 compared to the vehicle-treated group (Figure 4A). During the probe trial, vehicle-treated animals spent significantly less time in the target quadrant ($F(2,27)=22.02$, total n=30, $p<0.0001$). The percentage of time spent in the target quadrant in the treatment group was higher than the vehicle animals (Figure 4B). Swimming velocity was comparable among all the experimental groups. It suggested that the longer escape latency was due to the impaired learning and memory function, rather than the swimming ability (Figure 4C).

Annexin A1 exerted anti-inflammatory effect via FPR2/p38/COX-2 pathway

To assess the downstream signaling of Annexin A1, we treated the animals with FPR2 antagonist Boc2 and p38 MAPK inhibitor SB203580 and analyzed the downstream proteins at 24 hours after ICH. Consistent with our previous finding, phosphorylated p38 level was increased after ICH ($F(4,25)=55.51$, total n=30, $p<0.001$), which could potentially trigger downstream proinflammatory cascade. AnxA1 treatment effectively attenuated the induction p38. However, Boc2 abrogated these beneficial effects of AnxA1. The co-treatment of Boc2 and SB203580 also effectively attenuated this induction (Figure 5B). Phospholipase A2 ($F(4,25)=101.4$, total n=30, $p<0.0001$) and COX-2 ($F(4,25)=31.68$, total n=30, $p<0.0001$) levels were also significantly induced after ICH, suggesting more release of arachnoid acid

and more production of prostaglandins. Annexin A1 effectively attenuated this increase, which was again abolished by Boc2. Moreover, the cotreatment with p38 inhibitor SB203580 also significantly reduced PLA2 and COX-2 levels. This result suggested that p38 signaling might be in the upstream of proinflammatory arachnoid acid metabolites (Figure 5C and 5D). Proinflammatory cytokines IL-1β and TNF-α were also measured. Annexin A1 significantly reduced the cytokine levels compared to vehicle-treated animals ($F(4,25)=56.35$, total n=30, $p<0.0001$ in IL-1β; $F(4,25)=86.89$, total n=30, $p<0.001$ in TNF-α) while the co-treatment with Boc2 restored the cytokine levels. However, the co-treatment with SB203580 decreased the cytokine levels, indicating that p38 might be a downstream factor of AnxA1/FPR2 signaling (Figure 5E and Figure 5F).

Discussion

ICH is a stroke subtype with high mortality rate and no effective treatment is currently available. Mounting evidence has shown that inflammation, which begins immediately after the formation of hematoma, is one of the crucial contributors of ICH-induced secondary brain injury (Aronowski et al., 2011; Garton et al., 2017; Wang et al., 2018). In clinical settings, besides the surgical attempts to remove the hematoma after ICH takes place, corticosteroids were used to reduce inflammation and swelling. However, two clinical trials demonstrated that corticosteroids increased the mortality rates due to some unclear reason(Edwards et al., 2005; Roberts et al., 2004). The use of nonsteroidal anti-inflammatory drugs (NSAIDs) also remains controversial (Bak et al., 2003; Saloheimo et al., 2001). It has become critical for basic scientists to seek other anti-inflammatory treatments for ICH.

Annexin A1 has been shown to confer potential beneficial effects in preclinical stroke studies(Gavins et al., 2007; Wang et al., 2017). In this study, we administered exogenous Annexin A1 intracerebroventricularly after ICH and assessed its therapeutic effects, with a specific interest in brain edema, neurobehavioral outcomes and p38-related inflammatory response. Our data suggested that Annexin A1 attenuated brain edema at 24 hours and 72 hours after ICH, which mirrored the Garcia score at the same time points. This result was also in line with a previous study showing that Annexin A1 played a role in preserving blood-brain barrier after ICH. The mechanism involved two phosphorylation sites on Annexin A1 that maintained the cytoskeleton integrity on brain microvascular endothelial cells (Wang et al., 2017).

AnxA1 has been reported to be expressed on glial cells throughout the adult human and rodent brain, particularly on microglia (McArthur et al., 2010). Microglia are the resident immune cells in the central nervous system. They respond to immunological stimuli and secret pro-inflammatory cytokines (Aronowski et al., 2011). Our results suggested that microglia were activated after ICH as demonstrated by larger soma and that AnxA1 might attenuate microglial activation in the perihematoma area. However, Iba-1 positive cells might also include peripheral infiltrating macrophages. Gavins and colleagues previously demonstrated that AnxA1-induced stimulation of FPR2 decreased leukocyte adhesion to cerebral endothelial cells and reduced proinflammatory cytokine levels in a rodent model of

ischemia (Gavins et al., 2007). It is possible that AnxA1 also reduced peripheral macrophage infiltration by attenuating inflammatory response in the brain.

Several previous reports from our laboratory identified p38 MAPK as a detrimental factor in intracerebral hemorrhage as it contributed to inflammatory response and blood-brain barrier disruption(Chen et al., 2018; Ma et al., 2011). However, the upstream mechanisms still remain unclear. Recent data showed that AnxA1 could inhibit PLA2 activity and thus reduce arachidonic acid release and its downstream metabolites(Liu et al., 2007). In this study, we were trying to test whether AnxA1-FPR2 signaling could be a potential upstream candidate in inhibiting p38-triggered inflammatory cascade. Thus, we co-treated the animals with FPR2 inhibitor Boc-2 and p38 inhibitor SB203580 to see whether SB203580 could still mitigate the detrimental events after ICH even in the presence of FPR2 antagonism. Our data showed that the co-treatment with Boc-2 and SB203580 significantly reduced the protein levels of PLA2, COX-2, IL-1β and TNF-α compared to the vehicle treatment, meaning that p38 inhibition could significantly reduce inflammation even in the presence of FPR2 antagonism. However, animals receiving co-treatment of Boc-2 and SB203580 still have significantly higher levels of PLA2 and IL-1β compared to sham animals. This indicated that p38 inhibition partially, but not fully, mitigated the inflammatory response after ICH. There might be other pro-inflammatory mediators, not inhibited with SB203580, that trigger downstream inflammatory cascade. As for the further downstream factors, there could be other proinflammatory arachnoid acid metabolites produced independently of COX-2 activity, such as leukotrienes and 20-HETE. These lipid metabolites were not tested in this study and it would be intriguing to study their roles in future studies.

This study and several our previous papers indicated that ICH elicited acute inflammatory response, which may have a long-term impact on the memory function(Chen et al., 2018; Lu et al., 2019; Zhao et al., 2018). This current study focused on the expression profile of these signaling proteins at the acute phase. We did not expect the expression of these signaling proteins would be different at four weeks after ICH, when the inflammatory response is diminished. However, long-term structural or cellular changes, such as glial scar formation and decreased neuroplasticity, could sustain and might be attributed to the acute inflammatory response (Saulle et al., 2016). In clinical settings, long-term memory deficits are observed in ICH patients (P. Y. Garcia et al., 2013; Saulle et al., 2016; Xiong et al., 2016). However, the underlying mechanisms are still poorly understood. It is speculated that accumulation of amyloid precursor protein after ICH could contribute to memory loss and other types of cognitive impairment in the long term (Hijioka et al., 2016). However, further investigation and more evidence would be needed.

There are a few limitations with this study. First, we focused on the local immune response in the brain. We did not assess how the intracerebral administration of AnxA1 altered the peripheral immune response. Second, we focused on p38 MAPK in this study. Recent data have indicated that other MAPKs, such as ERK and JNK, may also have interplay with p38 in ICH (Chen et al., 2018). Whether and how ERK and JNK also play a role as the downstream factors of FPR2 signaling in the context of ICH remain to be investigated in future studies. Third, we only employed male mice in the current study. Although research data indicated that females are more protected due to estrogen in ICH(Nakamura et al.,

2005), it would still be critical to assess the therapeutic effects of AnxA1 in both premenopausal and postmenopausal females.

Supplementary Material

Refer to Web version on PubMed Central for supplementary material.

Other Acknowledgements

Grant information: This study is supported by an NIH grant R01-NS091042 to John H. Zhang.

Authors would like to thank Dr. Yan Peng for his assistance in performing some of the experiments.

References

Aronowski J, & Zhao X (2011). Molecular pathophysiology of cerebral hemorrhage: secondary brain injury. Stroke, 42(6), 1781–1786. doi:10.1161/STROKEAHA.110.596718 STROKEAHA. 110.596718 [pii] [PubMed: 21527759]

Bak S, Andersen M, Tsiropoulos I, Garcia Rodriguez LA, Hallas J, Christensen K, & Gaist D (2003). Risk of stroke associated with nonsteroidal anti-inflammatory drugs: a nested case-control study. Stroke, 34(2), 379–386.

Bena S, Brancaleone V, Wang JM, Perretti M, & Flower RJ (2012). Annexin A1 interaction with the FPR2/ALX receptor: identification of distinct domains and downstream associated signaling. J Biol Chem, 287(29), 24690–24697. doi:10.1074/jbc.M112.377101 [PubMed: 22610094]

Bromley-Brits K, Deng Y, & Song W (2011). Morris water maze test for learning and memory deficits in Alzheimer's disease model mice. J Vis Exp(53). doi:10.3791/2920

Carmichael ST, Vespa PM, Saver JL, Coppola G, Geschwind DH, Starkman S, … Martin NA (2008). Genomic profiles of damage and protection in human intracerebral hemorrhage. J Cereb Blood Flow Metab, 28(11), 1860–1875. doi:10.1038/jcbfm.2008.77 [PubMed: 18628781]

Chen S, Zhao L, Sherchan P, Ding Y, Yu J, Nowrangi D, … Zhang JH (2018). Activation of melanocortin receptor 4 with RO27-3225 attenuates neuroinflammation through AMPK/JNK/p38 MAPK pathway after intracerebral hemorrhage in mice. J Neuroinflammation, 15(1), 106. doi: 10.1186/s12974-018-1140-6 [PubMed: 29642894]

Cui YH, Le Y, Gong W, Proost P, Van Damme J, Murphy WJ, & Wang JM (2002). Bacterial lipopolysaccharide selectively up-regulates the function of the chemotactic peptide receptor formyl peptide receptor 2 in murine microglial cells. J Immunol, 168(1), 434–442. [PubMed: 11751990]

Dang G, Yang Y, Wu G, Hua Y, Keep RF, & Xi G (2017). Early Erythrolysis in the Hematoma After Experimental Intracerebral Hemorrhage. Transl Stroke Res, 8(2), 174–182. doi:10.1007/ s12975-016-0505-3 [PubMed: 27783383]

Degousee N, Stefanski E, Lindsay TF, Ford DA, Shahani R, Andrews CA, … Rubin BB (2001). p38 MAPK regulates group Ila phospholipase A2 expression in interleukin-1beta -stimulated rat neonatal cardiomyocytes. J Biol Chem, 276(47), 43842–43849. doi:10.1074/jbc.M101516200 M101516200 [pii] [PubMed: 11571275]

Edwards P, Arango M, Balica L, Cottingham R, El-Sayed H, Farrell B, … collaborators, C. t. (2005). Final results of MRC CRASH, a randomised placebo-controlled trial of intravenous corticosteroid in adults with head injury-outcomes at 6 months. Lancet, 365(9475), 1957–1959. doi:10.1016/ S0140-6736(05)66552-X [PubMed: 15936423]

Faber JE, Moore SM, Lucitti JL, Aghajanian A, & Zhang H (2017). Sex Differences in the Cerebral Collateral Circulation. Transl Stroke Res, 8(3), 273–283. doi:10.1007/s12975-016-0508-0 [PubMed: 27844273]

Garcia JH, Wagner S, Liu KF, & Hu XJ (1995). Neurological deficit and extent of neuronal necrosis attributable to middle cerebral artery occlusion in rats. Statistical validation. Stroke, 26(4), 627–634; discussion 635. [PubMed: 7709410]

Garcia PY, Roussel M, Bugnicourt JM, Lamy C, Canaple S, Peltier J, … Godefroy O (2013). Cognitive impairment and dementia after intracerebral hemorrhage: a cross-sectional study of a hospital-based series. J Stroke Cerebrovasc Dis, 22(1), 80–86. doi:10.1016/j.jstrokecerebrovasdis.2011.06.013 [PubMed: 22421024]

Garton T, Keep RF, Hua Y, & Xi G (2017). CD163, a Hemoglobin/Haptoglobin Scavenger Receptor, After Intracerebral Hemorrhage: Functions in Microglia/Macrophages Versus Neurons. Transl Stroke Res, 8(6), 612–616. doi:10.1007/s12975-017-0535-5 [PubMed: 28386733]

Gavins FN (2010). Are formyl peptide receptors novel targets for therapeutic intervention in ischaemia-reperfusion injury? Trends Pharmacol Sci, 31(6), 266–276. doi:10.1016/j.tips.2010.04.001 [PubMed: 20483490]

Gavins FN, Dalli J, Flower RJ, Granger DN, & Perretti M (2007). Activation of the annexin 1 counter-regulatory circuit affords protection in the mouse brain microcirculation. FASEB J, 21(8), 1751–1758. doi:10.1096/fj.06-7842com [PubMed: 17317721]

Gavins FN, & Hickey MJ (2012). Annexin A1 and the regulation of innate and adaptive immunity. Front Immunol, 3, 354. doi:10.3389/fimmu.2012.00354 [PubMed: 23230437]

Gavins FN, Hughes EL, Buss NA, Holloway PM, Getting SJ, & Buckingham JC (2012). Leukocyte recruitment in the brain in sepsis: involvement of the annexin 1-FPR2/ALX anti-inflammatory system. FASEB J, 26(12), 4977–4989. doi:10.1096/fj.12-205971 fj.12-205971 [pii] [PubMed: 22964301]

Go AS, Mozaffarian D, Roger VL, Benjamin EJ, Berry JD, Blaha MJ, … Stroke Statistics, S. (2014). Executive summary: heart disease and stroke statistics--2014 update: a report from the American Heart Association. Circulation, 129(3), 399–410. doi:10.1161/01.cir.0000442015.53336.12 [PubMed: 24446411]

Hijioka M, Anan J, Matsushita H, Ishibashi H, Kurauchi Y, Hisatsune A, … Katsuki H (2016). Axonal dysfunction in internal capsule is closely associated with early motor deficits after intracerebral hemorrhage in mice. Neurosci Res, 106, 38–46. doi:10.1016/j.neures.2015.10.006 [PubMed: 26511923]

Jiang B, Li L, Chen Q, Tao Y, Yang L, Zhang B, … Zhu G (2017). Role of Glibenclamide in Brain Injury After Intracerebral Hemorrhage. Transl Stroke Res, 8(2), 183–193. doi:10.1007/s12975-016-0506-2 [PubMed: 27807801]

Lee SJ, Heo SH, Ambrosius WT, & Bushnell CD (2018). Factors Mediating Outcome After Stroke: Gender, Thrombolysis, and Their Interaction. Transl Stroke Res, 9(3), 267–273. doi:10.1007/s12975-017-0579-6 [PubMed: 29067622]

Liu NK, Zhang YP, Han S, Pei J, Xu LY, Lu PH, … Xu XM (2007). Annexin A1 reduces inflammatory reaction and tissue damage through inhibition of phospholipase A2 activation in adult rats following spinal cord injury. J Neuropathol Exp Neurol, 66(10), 932–943. doi:10.1097/nen.0b013e3181567d59 [PubMed: 17917587]

Lu Z, Wang Z, Yu L, Ding Y, Xu Y, Xu N, … Zhang JH (2019). GCN2 reduces inflammation by p-eIF2alpha/ATF4 pathway after intracerebral hemorrhage in mice. Exp Neurol, 313, 16–25. doi:10.1016/j.expneurol.2018.12.004 [PubMed: 30529503]

Ma Q, Huang B, Khatibi N, Rolland W 2nd, Suzuki H, Zhang JH, & Tang J (2011). PDGFR-alpha inhibition preserves blood-brain barrier after intracerebral hemorrhage. Ann Neurol, 70(6), 920–931. doi:10.1002/ana.22549 [PubMed: 22190365]

Marini S, Morotti A, Ayres AM, Crawford K, Kourkoulis CE, Lena UK, … Anderson CD (2017). Sex differences in intracerebral hemorrhage expansion and mortality. J Neurol Sci, 379, 112–116. doi:10.1016/j.jns.2017.05.057 [PubMed: 28716219]

McArthur S, Cristante E, Paterno M, Christian H, Roncaroli F, Gillies GE, & Solito E (2010). Annexin A1: a central player in the anti-inflammatory and neuroprotective role of microglia. J Immunol, 185(10), 6317–6328. doi:10.4049/jimmunol.1001095 [PubMed: 20962261]

Nakamura T, Hua Y, Keep RF, Park JW, Xi G, & Hoff JT (2005). Estrogen therapy for experimental intracerebral hemorrhage in rats. J Neurosurg, 103(1), 97–103. doi:10.3171/jns.2005.103.1.0097 [PubMed: 16121980]

Roberts I, Yates D, Sandercock P, Farrell B, Wasserberg J, Lomas G, … collaborators, C. t. (2004). Effect of intravenous corticosteroids on death within 14 days in 10008 adults with clinically

significant head injury (MRC CRASH trial): randomised placebo-controlled trial. Lancet, 364(9442), 1321–1328. doi:10.1016/S0140-6736(04)17188-2 [PubMed: 15474134]

Roquer J, Rodriguez-Campello A, Jimenez-Conde J, Cuadrado-Godia E, Giralt-Steinhauer E, Vivanco Hidalgo RM, … Ois A (2016). Sex-related differences in primary intracerebral hemorrhage. Neurology, 87(3), 257–262. doi:10.1212/WNL.0000000000002792 [PubMed: 27281527]

Saloheimo P, Juvela S, & Hillbom M (2001). Use of aspirin, epistaxis, and untreated hypertension as risk factors for primary intracerebral hemorrhage in middle-aged and elderly people. Stroke, 32(2), 399–404. [PubMed: 11157173]

Saulle MF, & Schambra HM (2016). Recovery and Rehabilitation after Intracerebral Hemorrhage. Semin Neurol, 36(3), 306–312. doi:10.1055/s-0036-1581995 [PubMed: 27214706]

Strbian D, Durukan A, & Tatlisumak T (2008). Rodent models of hemorrhagic stroke. Curr Pharm Des, 14(4), 352–358. [PubMed: 18289061]

Wang Z, Chen Z, Yang J, Yang Z, Yin J, Zuo G, … Chen G (2017). Identification of two phosphorylation sites essential for annexin A1 in blood-brain barrier protection after experimental intracerebral hemorrhage in rats. J Cereb Blood Flow Metab, 37(7), 2509–2525. doi: 10.1177/0271678X16669513 [PubMed: 27634935]

Wang Z, Zhou F, Dou Y, Tian X, Liu C, Li H, … Chen G (2018). Melatonin Alleviates Intracerebral Hemorrhage-Induced Secondary Brain Injury in Rats via Suppressing Apoptosis, Inflammation, Oxidative Stress, DNA Damage, and Mitochondria Injury. Transl Stroke Res, 9(1), 74–91. doi: 10.1007/s12975-017-0559-x [PubMed: 28766251]

Xiong L, Reijmer YD, Charidimou A, Cordonnier C, & Viswanathan A (2016). Intracerebral hemorrhage and cognitive impairment. Biochim Biophys Acta, 1862(5), 939–944. doi:10.1016/j.bbadis.2015.12.011 [PubMed: 26692171]

Zhao L, Chen S, Sherchan P, Ding Y, Zhao W, Guo Z, … Zhang JH (2018). Recombinant CTRP9 administration attenuates neuroinflammation via activating adiponectin receptor 1 after intracerebral hemorrhage in mice. J Neuroinflammation, 15(1), 215. doi:10.1186/sl2974-018-1256-8 [PubMed: 30060752]

Significant Statement

No effective treatment strategies have yet been developed to ameliorate intracerebral hemorrhage (ICH) induced brain damage. Our goal of this study is to explore the therapeutic window, short-term and long-term effects of FPR2 activation in ICH induced brain damage and investigate the underlying mechanisms. Achieving our goal will lay the foundation for clinical evaluation of administration of AnxA1, an FPR2 agonist, in patients for the treatment of brain damage from ICH.

ICH elicits inflammatory response in the brain. Annexin A1/ FPR2 signaling attenuates neuroinflammation via inhibiting p38-associated inflammatory cascade.

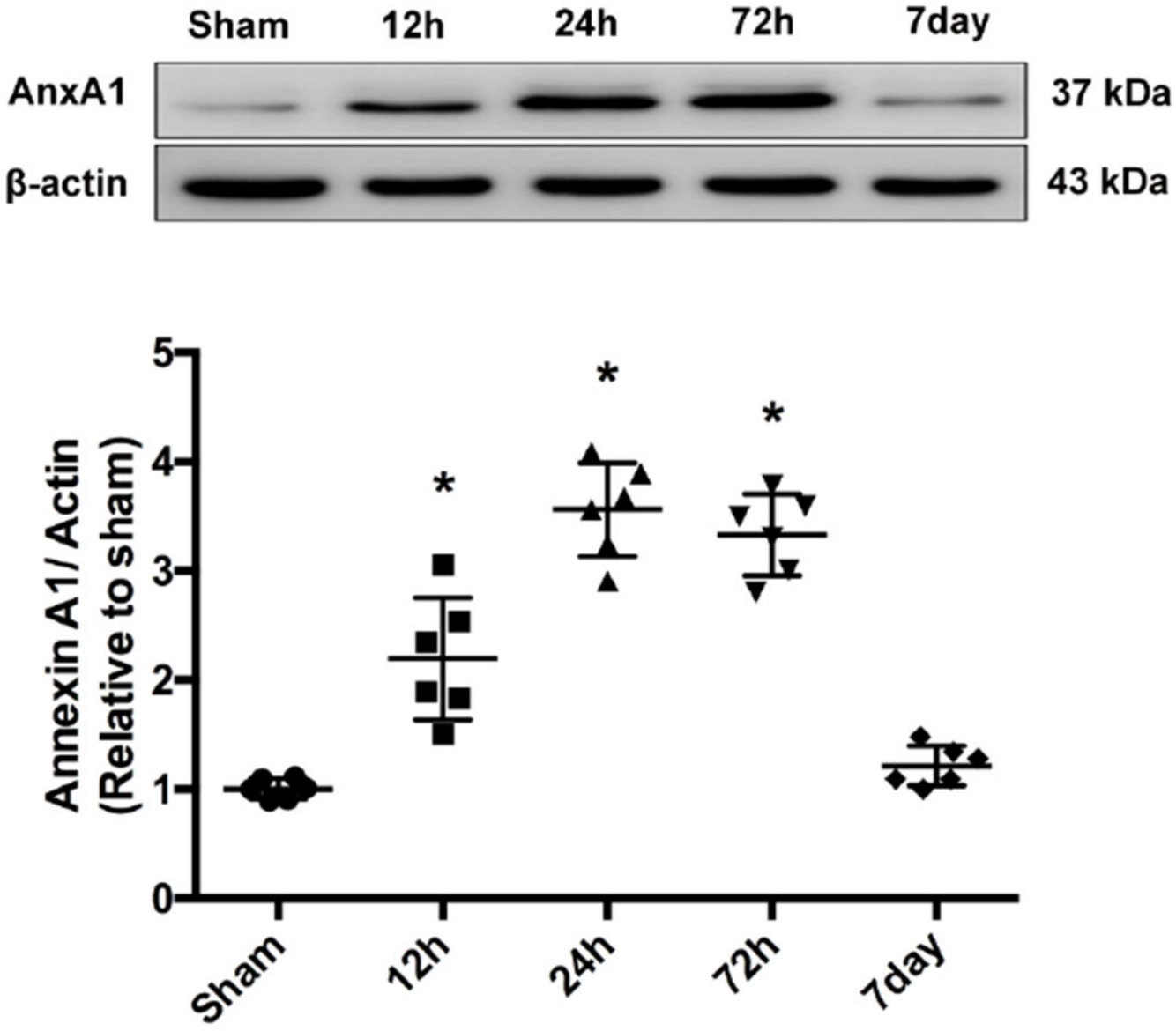

Figure 1.

Time course of endogenous AnxA1 expression after ICH. Representative Western blot bands and quantitative analyses of AnxA1 expression from ipsilateral hemispheres after ICH. *p<0.05 vs sham. Error bars are represented mean ± SD. One-way ANOVA, Tukey's test, n=6 per group.

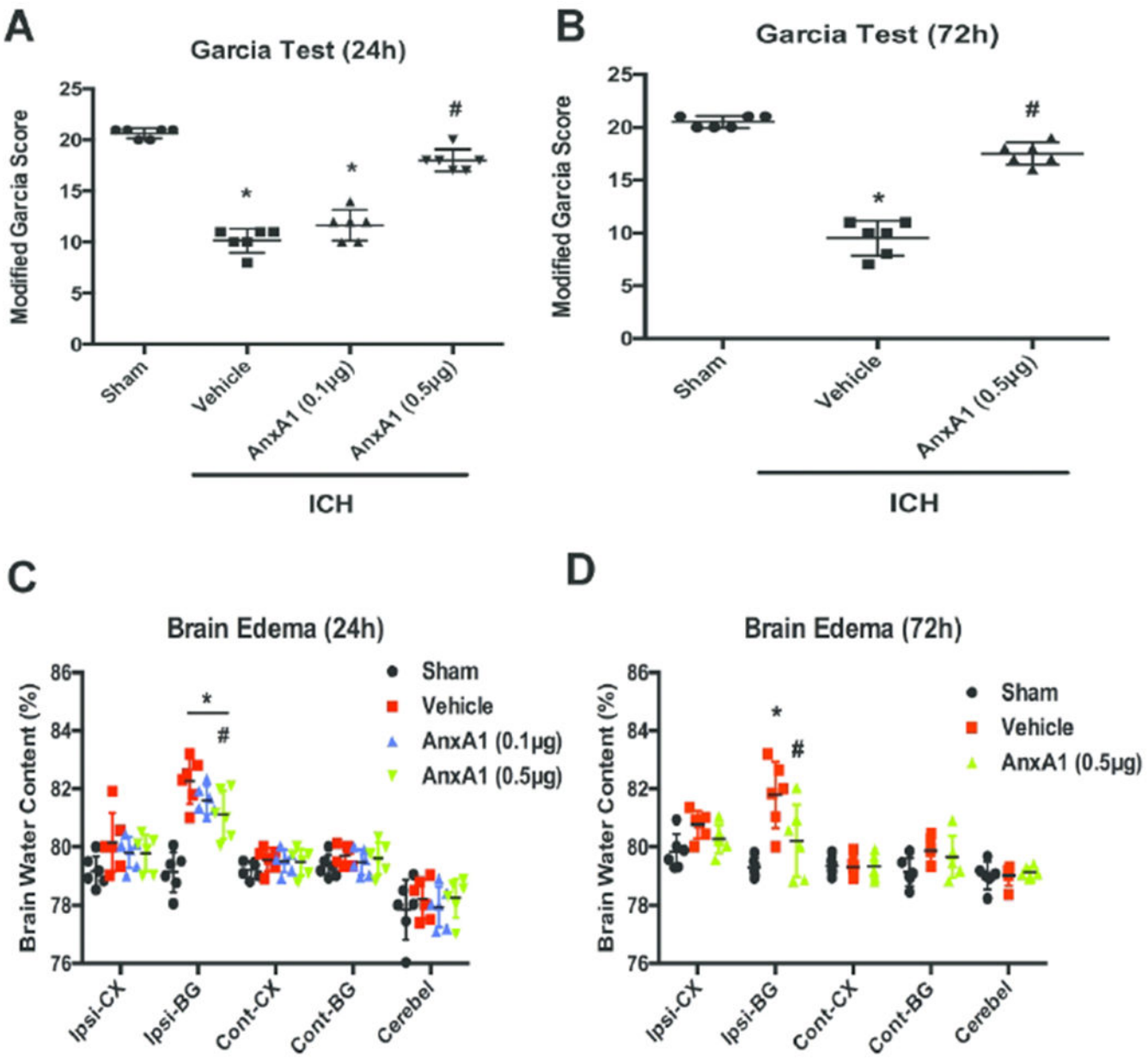

Figure 2.

AnxA1 improved neurological outcomes and attenuated brain edema at 24 and 72 hours after ICH in mice. A) Garcia Test at 24h, B) Garcia Test at 72h. C) Brain water content at 24 h, D) Brain water content at 72 h. Brains were divided into five parts: ipsilateral basal ganglia (ipsi-BG), ipsilateral cortex (ipsi-CX), contralateral basal ganglia (cont-BG), contralateral cortex (cont-CX), and cerebellum (cerebel). *p<0.05 vs. sham, $^{\#}p$<0.05 vs. vehicle. Error bars are represented mean ± SD. Garcia score results were analyzed by Kruskal–Wallis test, followed by Dunn's test. Brain water content results were analyzed by one-way ANOVA, Tukey's test, n=6 per group.

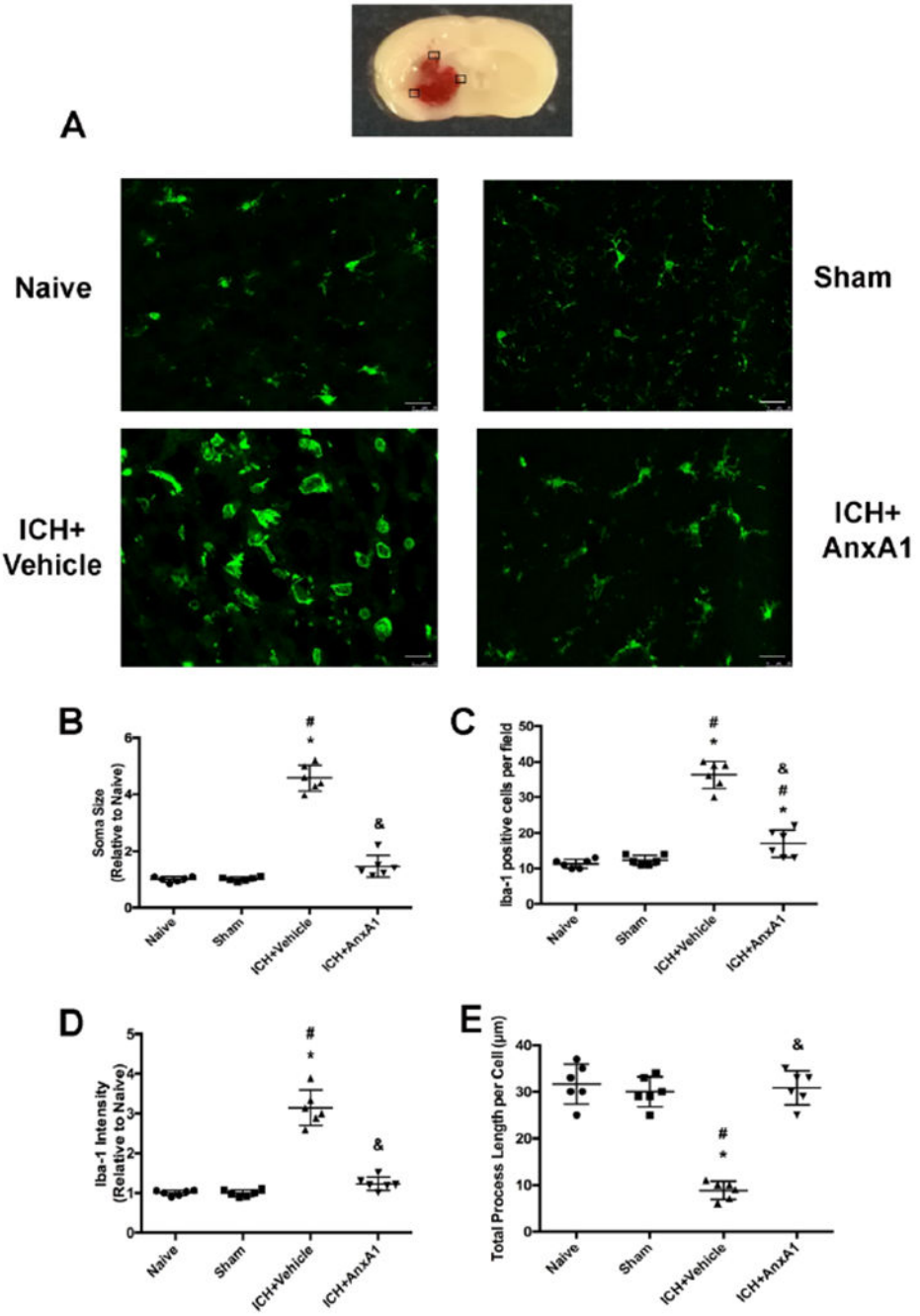

Figure 3.

Microglial activation in the perihematoma area of the brain at 24 hours after ICH. Microglia were stained with Iba-1 (red). A) Representative images of each experimental group. B) Soma size of microglia. C) Numbers of Iba-1 positive cells per field. D) Iba-1 fluorescence intensity. E) Total process length per cell (μm). Scale bar = 25μm. *p<0.05 vs. naïve, $^{\#}p$<0.05 vs. sham, $^{\&}$ p<0.05 vs. vehicle. Error bars are represented mean ± SD. One-way ANOVA, Tukey's test, n=6 per group.

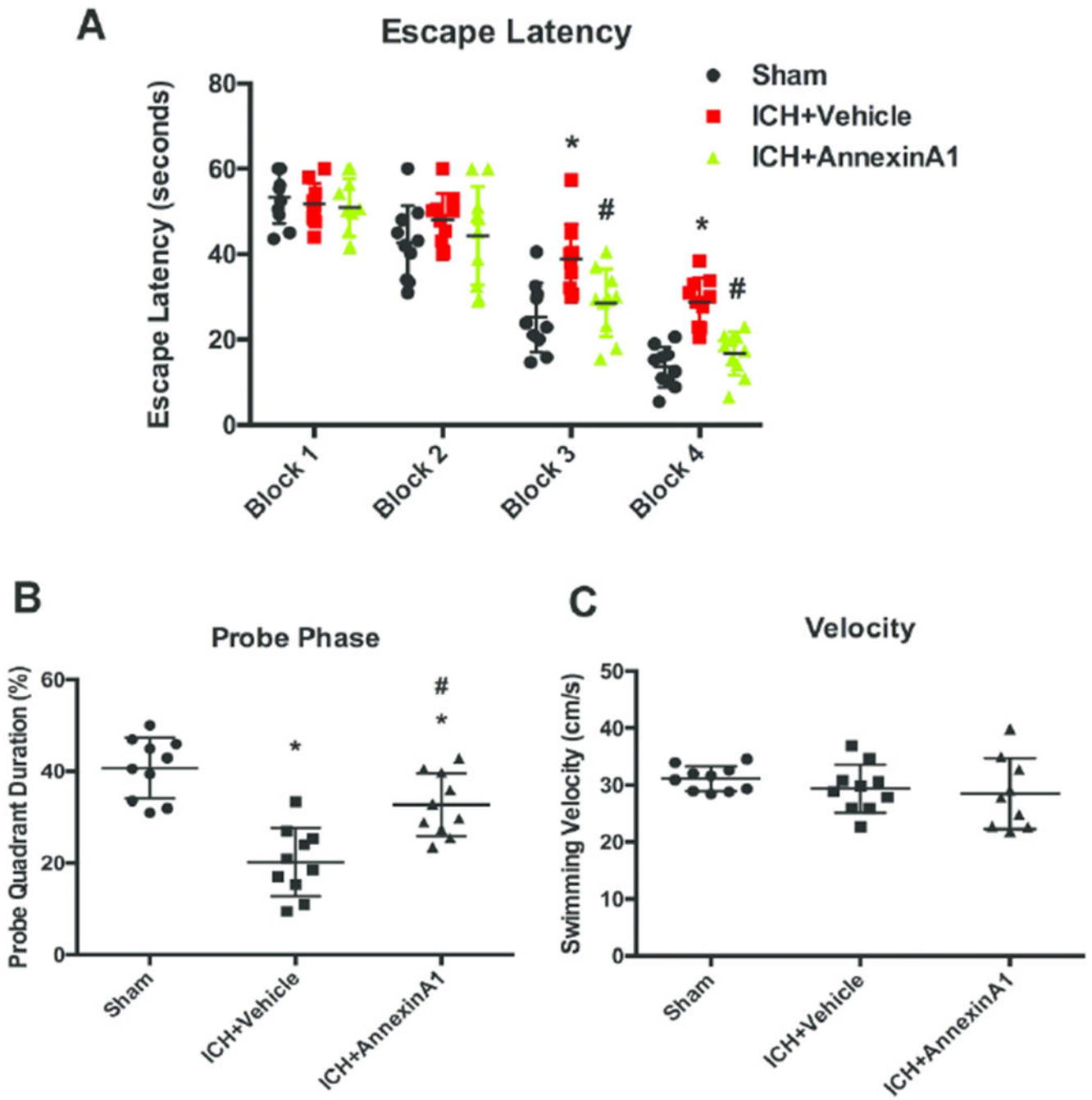

Figure 4.

AnxA1 improved memory function in Morris water maze. (A) Escape latency from Day 25 to Day 28 after ICH, (B) probe quadrant duration and (C) swimming velocity on Day 28 after ICH. *p<0.05 vs. sham, $^{\#}p$<0.05 vs. vehicle. Error bars are represented mean ± SD. Two-way ANOVA, Tukey's test for escape latency and one-way ANOVA, Tukey's test for probe quadrant duration and swimming velocity, n=10 per group.

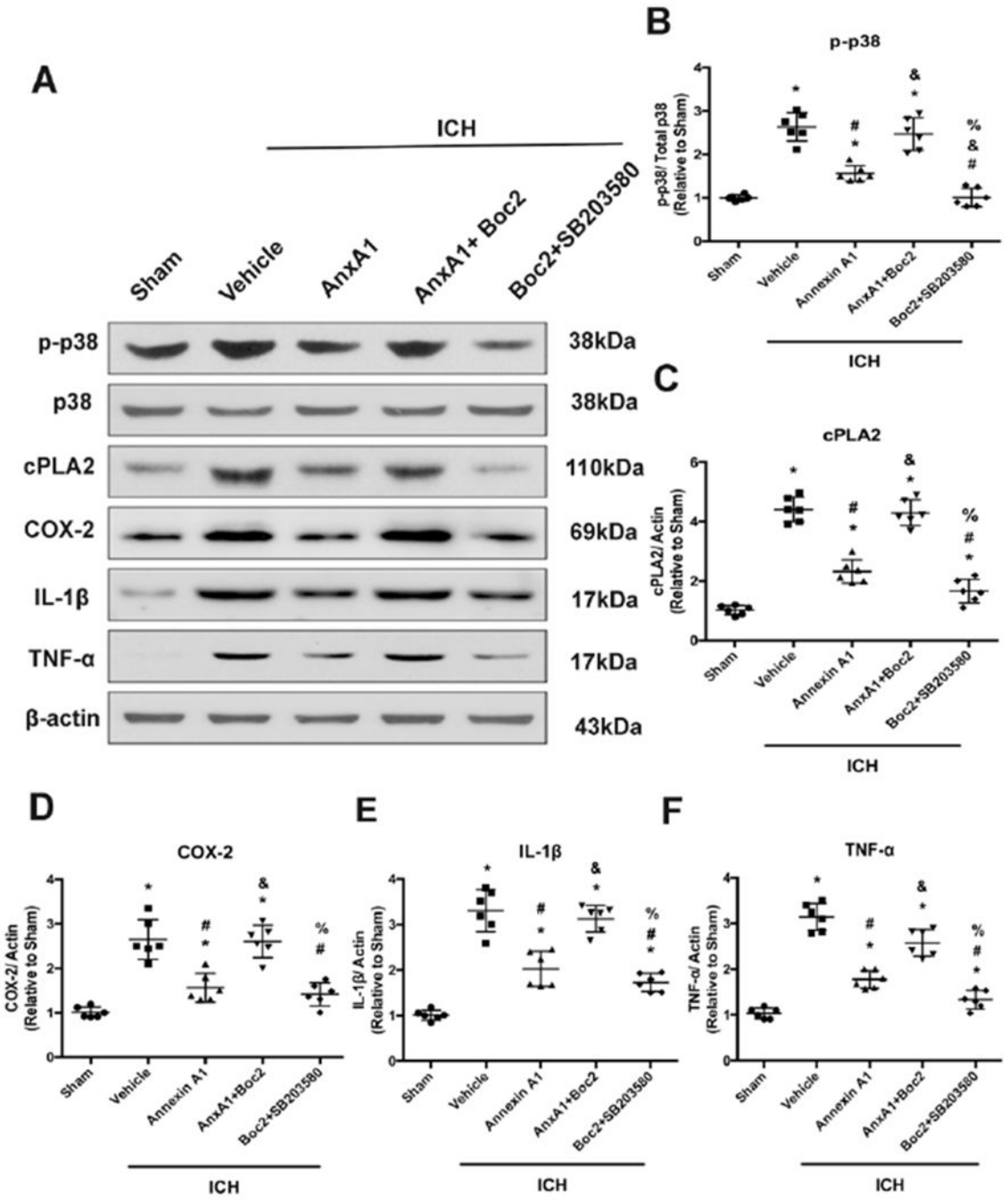

Figure 5.

AnxA1 conferred anti-inflammatory effects through FPR2/p38/COX-2 pathway. (A) Representative Western blot bands. (B-F) Quantitative analyses of phosphorylated p38, cPLA2, COX-2, TNF-α, and IL-1β in the ipsilateral hemisphere at 24h after ICH. *p<0.05 vs. sham, $^{\#}p$<0.05 vs. vehicle, $^{\&}p$<0.05 vs. AnxA1, $^{\%}p$<0.05 vs. AnxA1+Boc2. Error bars are represented mean ± SD. One-way ANOVA, Tukey's test, n=6 per group.

Table 1.

Information of antibodies in this study.

Antibody Table

Antibody	Immunogen Structure	Manufacturer	Catalog # and RRID	Species	Concentration
Annexin A1	Full length human recombinant	ThermoFisher Scientific	71-3400 AB_2533983	Rabbit polyclonal	1/1000
Iba-1	Human Ibal aa 1-100	Abcam	ab178847	Rabbit monoclonal	1/100
phosphorylated p38 (p-p38)	Thr180/Tyr182 of human p38 MAPK	Cell Signaling Technology	CST9211	Rabbit	1/1000
p38 MAPK	Synthetic peptide corresponding to the sequence of human p38 MAPK	Cell Signaling Technology	9212 AB_330713	Rabbit	1/1000
Cytosolic Phospholipase A2 (cPLA2)	Human cPLA2 phospho-S505	Abcam	ab58375 AB_881998	Rabbit polyclonal	1/1000
Cyclooxygenase-2 (COX-2)	Rat COX-2 aa550 to the C-terminus	Abcam	ab15191 AB_2085144	Rabbit polyclonal	1/1000
IL-1β	mouse IL-1β Val175	Cell Signaling Technology	CST12426	Rabbit monoclonal	1/1000
TNF-α	Recombinant full length protein	Abcam	ab6671 AB_305641	Rabbit polyclonal	1/1000
β-actin	C-terminus of human actin	Santa Cruz Biotechnology	sc1616 AB_630836	Goat Polyclonal	1/3000